In situ surface-enhanced Raman spectroscopy of monodisperse silver nanowire arrays

G. Sauer, G. Brehm, and S. Schneider
Institute of Physical and Theoretical Chemistry, University of Erlangen, Egerlandstrasse 3, D-91058 Erlangen, Germany

H. Graener and G. Seifert
Department of Physics, Martin-Luther University of Halle–Wittenberg, 06108 Halle, Germany

K. Nielsch, J. Choi, P. Göring, and U. Gösele
Max-Planck-Institute of Microstructure Physics, 06120 Halle, Germany

P. Miclea and R. B. Wehrspohn[a)]
Nanophotonic Materials Group, Department of Physics, University of Paderborn, 33095 Paderborn, Germany

(Received 23 July 2004; accepted 20 October 2004; published online 27 December 2004)

Highly ordered two-dimensional arrays of monodisperse coinage metal nanowires embedded in an alumina matrix have been prepared. When light is propagating in the direction of the long axis of the nanowire, plasmon-enhanced absorption and light guidance of the nanowire were observed by optical microspectroscopy and scanning near-field optical spectroscopy and compared to Mie scattering theory. By selectively dissolving the matrix at a constant etching rate, we detected *in situ* and *ex situ* the surface-enhanced Raman scattering (SERS) of organic dyes. In contrast to earlier publications, we find that the SERS signal is linearly proportional to the free-surface area of the nanowires that are in contact with the dye. We cannot detect any change in the enhancement factor due to the releasing of the nanowires from the host structure. © *2005 American Institute of Physics*. [DOI: 10.1063/1.1833580]

I. INTRODUCTION

Metal nanoparticles have gained considerable interest in the last years, both in basic research studying surface-plasmon polaritons as well as in applied research. For example, metal nanostructures have been proposed to enhance light emission of midinfrared sources[1] as well as light-emitting diodes,[2] to improve the resolution in spectroscopy and microscopy,[3] and to serve as passive optical devices such as filter.[4,5]

Another field of application for metal nanostructures is surface-enhanced Raman scattering (SERS) applied to the detection or sensing of ultralow concentrations of molecules.[6] When molecules are adsorbed at coinage metal nanoparticles, the Raman signal of the adsorbed species can be enhanced by factors on the order of 10^{14}–10^{15} due to the interaction with the nanoparticle enabling the detection of single molecules. This enormous enhancement is commonly explained by a combination of two mechanisms, namely, a minor contribution ($\leqslant 10^3$) from the charge-transfer (CT) mechanism and the major contribution ($\geqslant 10^6$) from the electromagnetic (EM) mechanism. Therefore, SERS measurements on well-defined nanoparticle systems are well suited to probe the local electromagnetic field in the vicinity of the nanoparticle. According to the EM theory, the enhancement of a given electromagnetic field in close vicinity of a nanoparticle critically depends on the nanoparticle's size, shape, and orientation towards the incoming field.[7] Most SERS systems are currently either based on roughened metal surfaces or colloidal metal particles. In both cases, the electromagnetic field enhancement cannot be easily determined.

To date, only a few studies concerning SERS on nanowires prepared in porous templates are published.[8–13] The templates used were disordered and had a wide pore size distribution and from the experimental details given, one can conclude that the homogeneity of the metal filling was quite poor. Therefore, the intensities of space-averaged SERS signals are likely to vary locally making the interpretation of the SERS data difficult. In contrast to the studies mentioned above, in our experiments we use highly ordered arrays of monodisperse nanowires with adjustable but well-defined diameter and length.

In this article, we first discuss in detail the optical properties of metal-filled highly ordered porous alumina. Based on these results, we present *ex situ* and *in situ* SERS measurements on these structures. In contrast to earlier publications,[14–17] the porous alumina templates in this work are 100% filled and the monodispersity of the wires has been improved dramatically since the discovery of the self-ordered growth regimes of porous alumina in 1997. Whereas disordered porous alumina templates have a coefficient of variation (CV) of the pore diameter of about 20%, self-ordered porous alumina has a CV of only 8%.

II. PREPARATION OF NANOWIRE ARRAYS

The preparation of highly ordered metal nanowire arrays is described in detail in Refs. 18 and 19. In a nutshell, hex-

[a)]Electronic mail: wehrspohn@physik.upb.de

TABLE I. Electrolytes used for nanowire preparation.

Metal	Electrolyte
Silver	$AgSO_4$, KSCN, $(NH_4)_2$H-citrate
Gold	$Na_3AuS_2O_3$, $(NH_4)_2$H-citrate
Copper	$CuSO_4$, $MgSO_4$, H_2SO_4

agonally ordered porous Al_2O_3 templates with an interpore distance of 110 nm are fabricated on aluminum substrates using a two-step electrochemical etching process. The templates have a pore diameter variation of less than 8% and the size of the ordered domains exceeds several micrometers. The pore diameter can be adjusted after anodization to its desired value by wet chemical etching in oxalic acid. Successive current-limited anodization yields small dendrite pores at the pore bottom which promote a homogeneous nucleation for the electrochemical metal deposition. Finally, metals are electroplated by pulsed electrodeposition onto the nearly insulating barrier oxide at the pore bottom. This technique is known to yield a homogeneous metal filling of high aspect-ratio pores. The used electrolyte is summarized in Table I.

For all described experiments, the nanowires had a diameter of about 40 nm and an initial length of approximately 2 μm corresponding to an aspect ratio of 50.

III. OPTICAL PROPERTIES OF NANOWIRE ARRAYS

The optical properties of ordered arrays of porous alumina have been studied by us in detail in Ref. 20. Porous anodic alumina is transparent in the whole visible spectral range similar to its crystalline counterpart. However, it is an optically inhomogeneous material consisting of cylindrical layers around the pores with varying refractive index. The variation is typically between $n=1.4$ and 1.7 and depends on the amount of anions locally incorporated in the alumina matrix. In this article, templates being homogeneously filled with a coinage metal have been studied with local optical transmission spectroscopy and near-field optical microscopy.

Local optical transmission spectroscopy in the visible spectral range has been conducted using a J & M TIDAS-MSP 400 microscope spectrometry system based on a Zeiss Axioplan 2 microscope. The light from a quartz tungsten halogen (QTH) lamp transmitted through the sample is, via an optical fiber, delivered into a spectral analyzer employing a 1024-element photodiode array and a data acquisition system with 16-bit resolution; the spectral resolution is 2 nm. With the help of an adjustable rectangular diaphragm in the back focal plane arbitrary sample areas can be studied; for this investigation, square areas of 30×30 μm were used. To extend the dynamic range of the data acquisition system, all the spectra shown here were recorded in a two-step procedure using appropriate spectral filters to match the emission characteristics of the light source to the extinction profile of each individual sample. In this way, reliable extinction spectra up to an optical density of 3.5 could be recorded in the range from 380 to 700 nm.

For the optical measurements, the filled template has been glued on a copper ring (inner diameter=1.5 mm) and

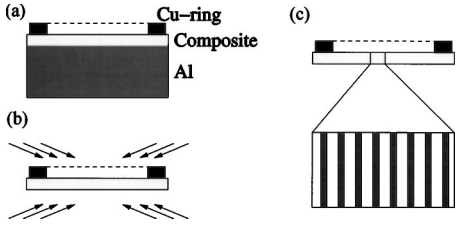

FIG. 1. Schematic illustration of the steps of the sample preparation: (a) a copper ring is glued on top of the filled alumina template, (b) after selectively removing the aluminum the top and the bottom side of the alumina membrane can be removed by ion milling, (c) the ion-milled template contains only nanowires; excessively deposited metal and the dentride strucure are removed completely.

the aluminum on the backside of the template has been selectively dissolved in a $CuCl_2$/HCl solution. Then, both sides of the filled template have been thinned by ion milling to remove the dendritic metal filling on the one side and possible metal deposition on the top of the template on the other side (Fig. 1). The ion-milling time determines the final thickness of the filled template. Figure 2 shows the typical extinction spectra of highly ordered ensembles of metal nanowires (Ag, Au, and Cu). The detection limit of our optical setup corresponds to an optical thickness of 3.5. The parameters are pore diameter $D_p\approx40$ nm and interpore distance $D_{\text{int}}\approx110$ nm. The propagation direction of the white light is perpendicular to the surface, i.e., parallel to the long axis of the nanowire. The electric field is, therefore, perpendicular to the long axis of the nanowire. A shift in the extinction maximum, i.e., plasmon resonance towards shorter wavelength, is observable from Cu over Au to Ag. This corresponds qualitatively to the resonance in the dielectric function of the corresponding bulk metals (Ag: $\lambda_{\text{max,bulk}}\approx445$ nm, Au: $\lambda_{\text{max,bulk}}\approx520$ nm, and Cu: $\lambda_{\text{max,bulk}}\approx570$ nm). We also performed calculation based on the Mie theory.[21] Since the electric field in this configuration is strictly perpendicular to the long axis of the wire, the generalized Lorenz–Mie theory can be applied. Figure 3 shows numerical simulations of the extinction spectra for spherical particles with $D_p=40$ nm embedded in a porous alumina matrix ($n=1.45$). The peak position as well as the shape and relative magnitude of the Cu and Au samples correspond qualitatively to the experimental results (Au: $\lambda_{\text{max,Mie}}$

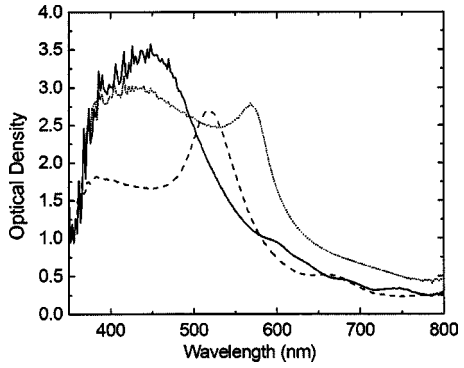

FIG. 2. Optically-determined extinction spectra for ordered silver (solid), gold (dashed), and copper (dotted) nanowire ensembles with pore diameter $D_p\approx40$ nm and interpore distance $D_{\text{int}}\approx110$ nm embedded in an alumina matrix.

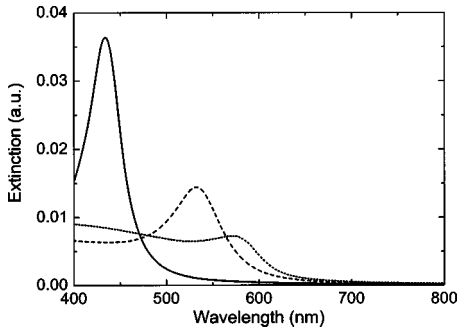

FIG. 3. Calculation extinction spectra for ordered silver (solid), gold (dashed), and copper (dotted) nanowire ensembles with pore diameter $D_p \approx 40$ nm and interpore distance $D_{\text{int}} \approx 110$ nm embedded in an alumina matrix ($n=1.45$).

≈ 530 nm and Cu: $\lambda_{\text{max,Mie}} \approx 575$ nm). For the Ag sample, the theoretically predicted optical thickness is at least a factor of 2 higher than that of Au or Cu with a maximum at $\lambda_{\text{max,Mie}} = 433$ nm. This corresponds to an optical thickness of about six in comparison with the experimental data of Au. Since the detection limit of our optical system is about 3.5, the maximum could not be detected.

Near-field optical microscopy of the samples was performed in an Alpha scanning near-field optical microscope (SNOM) purchased from WITec GmbH (Ulm, Germany). The Alpha SNOM uses micromachined cantilever SNOM sensors with an optical aperture of <80 nm at the tip, defining at the same time the spatial resolution of the system. For SNOM pictures the sample is scanned on a piezocontrolled *x*-*y*-*z* scanner, the cantilever being kept in contact with the sample surface adjusting the *z* position of the sample with the help of an optical beam deflection feedback. The probe light is focused into the aperture of the SNOM cantilever, and only the light transmitted through the aperture is registered. The experiments in this work were done in transmission mode, i.e., the near-field signal was collected by a microscope objective in a confocal position below the sample, and then monitored by a single-photon-counting photomultiplier tube.

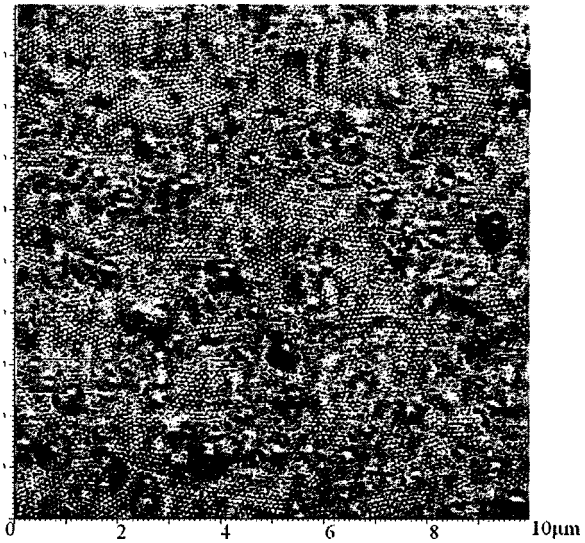

FIG. 4. Near-field optical transmission measurement of the Ag sample illuminated with a He–Ne laser ($\lambda = 632.8$ nm).

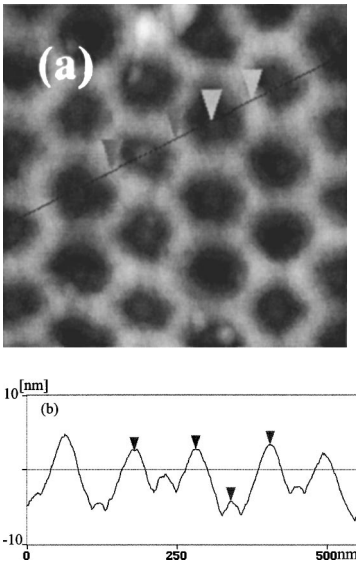

FIG. 5. Atomic force microscopy (AFM) images of the ion-milled Al_2O_3 templates filled with silver nanowires. (a) top view and (b) height profile along the line depicted in (a).

The picture shown in Fig. 4 refers to a probe wavelength of 632.8 nm (laser diode) and clearly shows the regular arrangement of the silver nanorods, where the optical contrast is caused by the different absorption coefficients at 632.8 nm of silver and matrix. White corresponds to a high transmission of light and black to a low transmission of light. As expected, light is mainly emitted by the surface-plasmon polaritons of the nanowires. Artifacts due to surface roughness can be excluded, since the simultaneously measured topography of the same sample area shows no indication of regular structures similar to the ones observed in the SNOM data.

IV. SURFACE-ENHANCED RAMAN SPECTROSCOPY

Prior to the SERS experiments, metal deposited in excess on the top of the template was removed by ion milling. By employing this procedure, it was ensured that highly uniform samples are obtained. Due to its high SERS enhancement factor, silver is the most frequently applied metal in SERS spectroscopy. Therefore, the experiments described in this contribution were conducted with silver nanowire ensembles. SERS spectra were taken either with a homebuilt Raman microscope [excitation wavelength $\lambda_{\text{exc}} = 632.8$ nm, laser power $\leqslant$ max 5 mW at the sample, microscope lens: 50×, NA 0.5 (allowing a spatial resolution of a few microns)] or with a Renishaw Raman microscope, System 2000 [$\lambda_{\text{exc}} = 514.5$ nm, laser power $\leqslant$ max 5 mW at the sample, microscope lens: 50×, NA 0.5 (allowing a spatial resolution of ~ 1 μm)].

A. Nanowires embedded in the template

First, SERS experiments were performed with the composite samples obtained directly by ion milling. The typical topography of such a sample is displayed in Fig. 5. Almost all pores of the alumina matrix are filled with metal nanowires. Due to the ion-milling process—metal is easily re-

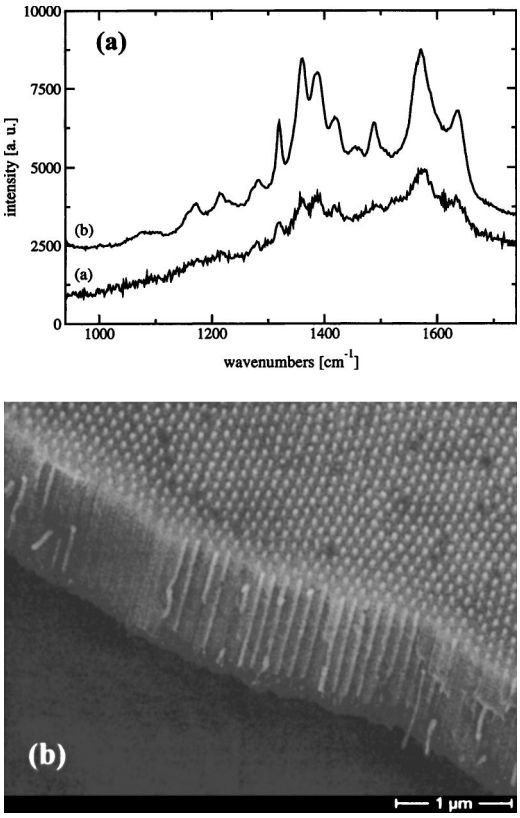

FIG. 6. (a) SERS spectra of proflavine measured at (a) nanowires embedded in the template and (b) at a site of fracture with $\lambda_{exc}=514.5$ nm, (b) SEM micrograph (side view) of a fracture.

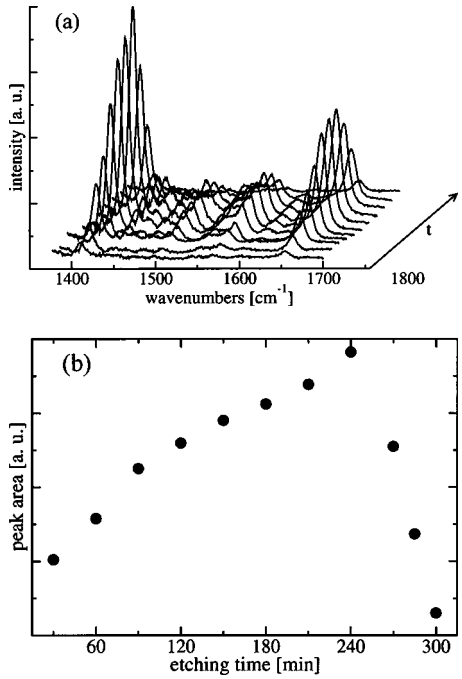

FIG. 7. (a) SERS spectra of oxazine 170 recorded with $\lambda_{exc}=632.8$ nm during an etching process, (b) plot of the SERS intensity vs the etching time.

moved by the ion-milling process as in the case of alumina—the nanowires end a few nanometers below the template matrix.

The samples were immersed in a 10^{-5} M aqueous solution of proflavine and afterwards rinsed with copious amounts of doubly distilled water to remove weakly bound adsorbates. Measuring the SERS spectra on well-controlled surfaces like the one shown in Fig. 5 usually yields reproducible spectra with relatively small signal intensity [Fig. 6(a)]. Because the Raman signal intensity is rather low one must conclude that the enhancement factor is low despite the large aspect ratio of the nanoparticles. This is not surprising, considering the orientation of the well-separated particles relative to the incident field and the low accessible surface only at the ends of the nanowires. However, at occasional sites of fracture [Fig. 6(b)], which typically evolve during sample pretreatment, SERS spectra with low as well as with very high signal intensity can be recorded depending on the location of the laser focus.

These results as well as those of other authors[8,10] suggest that higher SERS signal intensities can be observed, if the silver nanowires are (at least partially) released from the supporting template structure.

B. *In situ* SERS spectroscopy

To verify the hypothesis outlined above, the alumina matrix was selectively etched in a well-controlled manner by adding phosphoric acid to a solution containing the test dye oxazine 170. At the same time, the etching process was followed *in situ* with SERS spectroscopy (Fig. 7). In the beginning, the wires are completely embedded in the template structure and only the tips of the wires with a small surface area are available for adsorption of dye molecules. Therefore, as described above, the Raman signal intensity is rather low. With increasing etching time the silver wires are successively freed from the template and the SERS intensity increases up to a certain maximum. Scanning electron microscope (SEM) images taken from the samples after different etching times (not shown here) reveal that the nanowires are keeping their orientation almost parallel to the incident field at least at the beginning of the etching procedure. After passing the maximum the SERS intensity abruptly decreases. The SEM images indicate that after long etching times a complete dissolution of the alumina matrix causes the wires to collapse, form sheaves, or to be washed out from the substrate.

C. *Ex situ* SERS spectroscopy

In principle, different explanations can be given for the observed experimental results discussed so far. The most intuitive one is that the number of SERS active surface sites at the nanowires increases linearly with the etching time. However, Yao *et al.*[10] interpreted similar measurements on disordered metal nanowires arrays with the lightning rod effect.[22] According to this theory, the electromagnetic field enhancement at the tip increases with the aspect ratio of the wire.

Therefore, to gain further information about the enhancement properties of the nanowire ensembles the following *ex situ* SERS experiments (i.e., the test dye is not present during the etching process) were undertaken.

In the first experiment (Fig. 8), a sample was immersed in a 10^{-5} M aqueous solution of oxazine 170 and rinsed thoroughly with doubly distilled water and methanol to remove

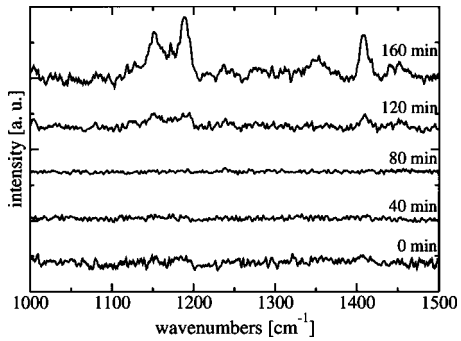

FIG. 8. SERS spectra of oxazine 170 adsorbed only at the tips of the nanowires after different etching times (λ_{exc}=632.8 nm).

weakly bound adsorbates. Although oxazine 170 is known to adsorb strongly at silver surfaces and, therefore, one can assume that there are dye molecules present at the tips of the nanowires, the SERS spectrum obtained from the dried sample contains no Raman bands attributable to oxazine. After measuring this spectrum, the sample is repeatedly incubated in 8% H_3PO_4 containing no oxazine 170 to selectively etch the alumina template and SERS spectra were recorded after each etching step. Only after relatively long etching times weak SERS bands of the dye molecules adsorbed at the tips of the nanowires evolve. Further etching causes the nanowires to be destabilized and to be released from the template. The SERS intensity abruptly decreases (not shown).

In a second experiment (Fig. 9), a sample was treated similar to the first experiment in the beginning. The SERS spectra recorded after a first etching step of 80-min duration exhibit the same lack of presence of oxazine Raman bands. In contrast to the first experiment, the sample was immersed a second time into the 10^{-5} M aqueous solution of oxazine 170. After rinsing and drying the sample intense SERS bands of oxazine emerge. Upon further etching in 8% H_3PO_4 the intensity of the bands increases until the alumina is dissolved and the nanowires are destabilized and washed out. The SERS signal intensity finally drops (not shown). The maximum intensity obtained in this second experiment is about two orders of magnitude higher than that obtained in the first *ex situ* experiment.

Since the increase in SERS intensity and the increase in the area of silver surface uncovered through cleavage are of the same order of magnitude, we believe that the gain or loss in the signal intensity can simply be related to the total silver surface area which is available for adsorption of the test dye. A higher surface area leads to a higher number of adsorbed molecules which results in a higher signal intensity. This explanation is also supported by Fig. 6. In the SEM micrograph, some cleaved pores are filled with silver wires (where we assume a high signal intensity) and some parts are almost empty (low signal intensity). We exclude any resonant Raman effects of the dye since the oxazine fluorescence intensity remains unchanged during the measurement.

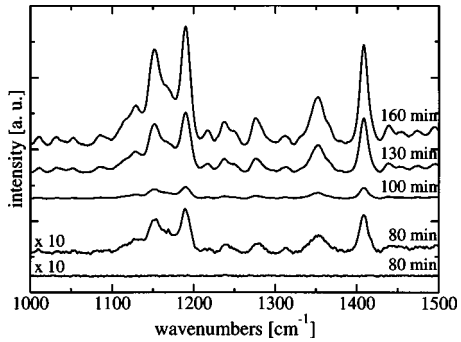

FIG. 9. Bottom trace: SERS spectrum of oxazine 170 adsorbed only at the tips of the nanowires after 80-min etching; other traces: SERS spectra of oxazine 170 adsorbed at the tips and at the sidewalls of the nanowires after different etching times (λ_{exc}=632.8 nm).

Two alternative interpretations for the observed loss in SERS intensity at longer etching times are possible. It could either be related to the reorientation and/or agglomeration of the silver wires reducing the SERS activity, or simply related to a loss of SERS active surface area in the laser spot due to detachment of wires.

V. CONCLUSION

In summary, we have prepared very well-controlled two-dimensional (2D) arrays of hexagonally arranged, monodisperse metal nanowires embedded in an alumina matrix. The dimensions of the nanowires can be adjusted by the template (wire diameter and length). The optical properties of these nanowire arrays have been determined by extinction spectra and near-field optical measurements. The plasmon bands of Au, Ag, and Cu have been observed and compared to Mie scattering models.

By selectively dissolving the matrix at a constant etching rate, we detected *in situ* and *ex situ* the surface-enhanced Raman scattering (SERS) of organic dyes. We found that the SERS signal is proportional to the free-surface area of the nanowires that are in contact with the dye. We cannot detect any change in the enhancement factor due to the releasing of the nanowires from the host structure. This model system is very useful in studying the impact of the different contributions to SERS enhancement and might be applied for diagnostic purposes in chemistry and biology.

[1]S. Y. Lin, J. Moreno, and J. G. Fleming, Appl. Phys. Lett. **83**, 380 (2003).
[2]A. Scherer, O. Painter, J. Vuckovic, M. Loncar, and T. Yoshie, IEEE Trans. Nanotechnol. **1**, 4 (2002).
[3]A. Hartschuh, E. J. Sanchez, X. S. Chie, and L. Novotny, Phys. Rev. Lett. **90**, 095503 (2003).
[4]S. Nonaka, T. Suda, and H. Oda, Jpn. J. Appl. Phys., Part 1 **41**, 4538 (2002).
[5]M. Kaempfe, H. Graener, A. Kiesow, and A. Heilmann, Appl. Phys. Lett. **79**, 1876 (2001).
[6]K. Kneipp, H. Kneipp, I. Itzkan, R. R. Dasari, and M. S. Feld, J. Phys.: Condens. Matter **14**, R 597 (2002).
[7]C. L. Haynes and R. P. Van Duyne, J. Phys. Chem. B **105**, 5599 (2001).
[8]Y. Joo and J. S. Suh, Bull. Korean Chem. Soc. **16**, 808 (1995).
[9]J. S. Suh and J. S. Lee, Chem. Phys. Lett. **281**, 384 (1997).
[10]J. L. Yao *et al.*, Pure Appl. Chem. **72**, 221 (2000).
[11]J. L. Yao *et al.*, Chem. Commun. (Cambridge) p. 1627 (2000).
[12]Z. Q. Tian, B. Ren, and D. Y. Wu, J. Phys. Chem. B **106**, 9463 (2002).
[13]J. L. Yao, J. Tang, D. Y. Wu, D. M. Sun, K. H. Xue, B. Ren, B. W. Mao, and Z. Q. Tian, Surf. Sci. **514**, 108 (2002).
[14]C. A. Foss, G. L. Hornyak, J. A. Stockert, and C. R. Martin, J. Phys. Chem. **96**, 7497 (1992).
[15]C. A. Foss, G. L. Hornyak, J. A. Stockert, and C. R. Martin, J. Phys. Chem. **98**, 2963 (1994).
[16]C. K. Preston and M. Moskovits, J. Phys. Chem. **97**, 8495 (1993).
[17]G. L. Hornyak and C. R. Martin, Thin Solid Films **303**, 84 (1997).

[18]K. Nielsch, F. Müller, A. P. Li, and U. Gösele, Adv. Mater. (Weinheim, Ger.) **12**, 582 (2000).
[19]G. Sauer, G. Brehm, S. Schneider, K. Nielsch, R. B. Wehrspohn, J. Choi, H. Hofmeister, and U. Gösele, J. Appl. Phys. **91**, 3243 (2002).
[20]J. Choi, Y. Luo, R. B. Wehrspohn, R. Hillebrand, J. Schilling, and U. Gösele, Appl. Phys. Lett. **83**, 3036 (2003).
[21]U. Kreibig and M. Vollmer, *Optical Properties of Metal Clusters* (Springer, Berlin, 1995).
[22]J. Gersten and A. Nitzan, J. Chem. Phys. **73**, 3023 (1980).